Heavy p-type carbon doping of MOCVD GaAsP using CBrCl$_3$

CrossMark

Christopher Heidelberger *, Eugene A. Fitzgerald

Department of Materials Science and Engineering, Massachusetts Institute of Technology, Cambridge, MA 02139, USA

ABSTRACT

CBrCl$_3$ is shown to be a useful precursor for heavy p-type carbon doping of GaAs$_x$P$_{1-x}$ grown via metalorganic chemical vapor deposition (MOCVD) across a range of compositions. Structural and electrical properties of the GaAsP films were measured for various processing conditions. Use of CBrCl$_3$ decreased the growth rate of GaAsP by up to 32% and decreases x by up to 0.025. The dependence of these effects on precursor inputs is investigated, allowing C-doped GaAsP films to be grown with good thickness and compositional control. Hole concentrations of greater than 2×10^{19} cm^{-3} were measured for values of x from 0.76 to 0.90.

© 2016 Elsevier B.V. All rights reserved.

1. Introduction

GaAs$_x$P$_{1-x}$ is a ternary III–V semiconductor which has found many uses. Since the early 1970s, it has been widely used to fabricate red, orange, and yellow light emitting diodes [1,2]. It was studied for use as a graded base layer in heterojunction bipolar transistors (HBTs) in the 1990s [3]. More recently, GaAsP has become a material of interest for the high-bandgap cell in multi-junction photovoltaic systems [4–6]. For III–V on Si applications, it is useful because it is a miscible alloy and nearly bridges the entire gap in lattice constant between Si and GaAs. Metalorganic chemical vapor deposition (MOCVD) has been the method of choice for most commercial growth of GaAsP and other III–V semiconductors.

Heavy p-type doping of GaAsP in excess of 1×10^{19} cm^{-3} is required in several device elements, such as Ohmic contact layers, tunnel junctions, and the base regions of HBTs. Carbon has an advantage over group II p-type dopants in its lower diffusivity [7] and higher solid solubility in GaAs [8]. There are several ways of doping with C in MOCVD. Various hydrocarbon sources have been used, including the methyl group from TMGa, but these generally require low growth temperatures and/or low V/III ratios and therefore result in a high density of deep-level traps and bad surface morphology [9,10].

CBrCl$_3$ and other halomethanes allow higher growth temperatures and V/III ratios so high-quality C-doped films can be grown [11]. However, they create reactive byproducts which can have two adverse effects on GaAs$_x$P$_{1-x}$ growth: substantial growth

rate reduction [12] and composition shift (change in x) [13]. Control over growth rate and composition is critical for device fabrication; therefore, it is important that we are able to understand the effect of C doping by CBrCl$_3$ on these parameters. In this paper, we report the thicknesses, compositions, and electrical properties of various C-doped GaAsP films.

2. Experiments

The epitaxial samples were prepared in a Thomas Swan/Aixtron cold-walled $6 \times 2''$ MOCVD reactor, with a close-coupled showerhead configuration. Trimethylgallium (TMGa) was used as a Ga precursor and AsH$_3$ and PH$_3$ were used as group V precursors. In the 1980s, CCl$_4$ was originally used as a C precursor for MOCVD GaAs [11], but is now unavailable for environmental reasons. Replacing one or more Cl atoms with Br yields compounds which are potential candidates; however, of these only CBrCl$_3$ is a liquid at room temperature, an important criterion for bubbler design. Hence, in this study CBrCl$_3$ was used as a C precursor, with a bubbler temperature of 26 °C. The total reactor pressure for all samples was 100 Torr, with N$_2$ used as carrier gas. Susceptor rotation speed was 100 rpm.

Samples were grown with a structure shown in Fig. 1. Si substrates were used for all GaAsP samples because tensile GaAsP films grown on GaAs substrates had a tendency to crack, yielding inaccurate Hall effect measurements. N-type (100) Si substrates with a 6° offcut were used. The offcut is necessary to obtain single-domain GaAsP [14]. Si$_{0.5}$Ge$_{0.5}$ was grown via a Si$_{1-y}$Ge$_y$ graded buffer using a vertical-tube UHVCVD reactor. The wafers were then chemical-mechanically polished to remove surface roughness [15]. Next, in the MOCVD reactor, a Si$_{1-y}$Ge$_y$ graded buffer was grown
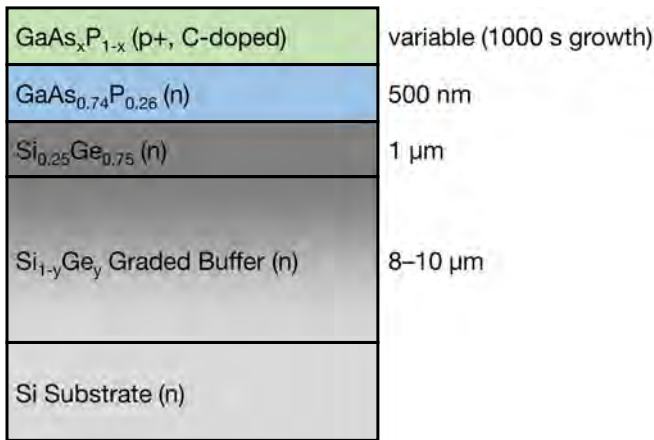
Fig. 1. Cross-sectional schematic of the epitaxial samples.

from $y=0.5$ to $y=0.75$, upon which an n-type $GaAs_{0.74}P_{0.26}$ film was initiated at 725 °C and grown to 500 nm. Then, under a mixed AsH_3 and PH_3 overpressure, the growth temperature was lowered to the final growth temperature (600 °C or 650 °C). A C-doped GaAsP film was then deposited for 1000 s with a TMGa flow of 132 µmol/min and a V/III ratio of about 100. The C-doped GaAs and GaP films were grown directly on their respective n-type substrates rather than on Si.

Table 1 shows a summary of the process conditions for all of the C-doped GaAsP films, grown at a variety of temperatures, $CBrCl_3$ flow rates, and AsH_3 fractions. AsH_3 fraction, the chosen metric of As precursor in the gas phase, is defined as:

$$AsH_3 \quad \text{Fraction} = \frac{P_{AsH_3}}{P_{AsH_3} + P_{PH_3}}, \tag{1}$$

where P_{AsH_3} and P_{PH_3} are the input partial pressures of AsH_3 and PH_3, respectively.

Sample A was grown at a temperature of 650 °C, while all other samples were grown at 600 °C. Samples B–F vary AsH_3 fraction, and therefore the solid $GaAs_xP_{1-x}$ composition, while keeping a constant $CBrCl_3$ flow. Samples G, C, and H vary the $CBrCl_3$ flow with a constant AsH_3 fraction. Sample J has multiple GaAsP layers with varying AsH_3 fractions and no $CBrCl_3$ flow. The AsH_3 fractions of 0.18–0.37 were chosen because at a growth temperature of 600 °C, they result in GaAsP compositions which span most of the direct band gap range [16]. The V/III ratio was kept constant while varying AsH_3 fraction.

Layer thicknesses were measured using cross-sectional SEM. High-resolution x-ray diffraction was used to measure film composition. (004) and (224) reciprocal space maps of the film and substrate were collected and used to find the in-plane and out-of-plane lattice constants of the C-doped GaAsP film using the methodology described in detail in Section 3.1 of Roesener et al. [17]. These values allowed for estimation of the relaxed lattice

Table 1
List of GaAsP samples with growth conditions.

Sample ID	Temperature (°C)	CBrCl$_3$ flow (µmol/min)	AsH$_3$ fraction
A	650	118	0.53
B	600	59	0
C	600	59	0.18
D	600	59	0.27
E	600	59	0.37
F	600	59	1
G	600	15	0.18
H	600	118	0.18
J	600	0	0.18, 0.27, 0.37

constant, using a Poisson ratio interpolated from the GaP and GaAs endpoints. The As content of the film was then calculated by Vegard's law. Hall effect measurements used the van der Pauw geometry and a permanent magnet with a field of 0.412 T. Indium was used to make contact to the GaAsP film. Given the finite size of the contacts, an error in Hall effect voltage of 5% was estimated [18]. Because of the pronounced effect of $CBrCl_3$ on GaAsP growth rate, the individually measured thickness of each sample was used in calculating its bulk carrier concentration. Leakage current into the n-type buffer layers and substrate was measured for representative Hall effect structures. Reverse bias leakage current from the p-doped GaAsP film into the n-doped substrate was less than 0.1% of the current between two Hall effect terminals at the same voltage. Therefore, any contribution of the n-type substrate to the sheet resistance or Hall voltage measurements was deemed to be insignificant. C concentration in Sample H was measured using secondary ion mass spectrometry (SIMS), which was performed by Evans Analytical Group.

3. Results and discussion

3.1. Effect of growth temperature

Sample A, grown at 650 °C, yielded a hole concentration of 9×10^{17} cm^{-3}. This is too low for the applications discussed in Section 1. Growth temperatures of 650 °C and higher are preferred for MOCVD growth of GaAsP. This is due to increased concentrations of impurities at lower temperatures as well as decreased PH_3 cracking efficiency [19,20]. However, it is known that a decreased growth temperature of 600 °C or lower produces the highest hole concentrations in C-doped GaAs [11,12]. Sample H, grown with the same $CBrCl_3$ flow rate as Sample A but at 600 °C, yielded a hole concentration of 2×10^{19} cm^{-3}. This confirms that the active C doping of GaAsP also increases with decreasing growth temperature. The rest of this study focuses on a growth temperature of 600 °C because growth temperatures less than 600 °C are undesirable for the reasons mentioned above.

3.2. Growth rate reduction by CBrCl$_3$

The growth rate of GaAsP was decreased by the introduction of $CBrCl_3$. Fig. 2 shows the growth rate reduction for a single AsH_3 fraction (0.18) as a function of $CBrCl_3$ flow. Lee et al. model the
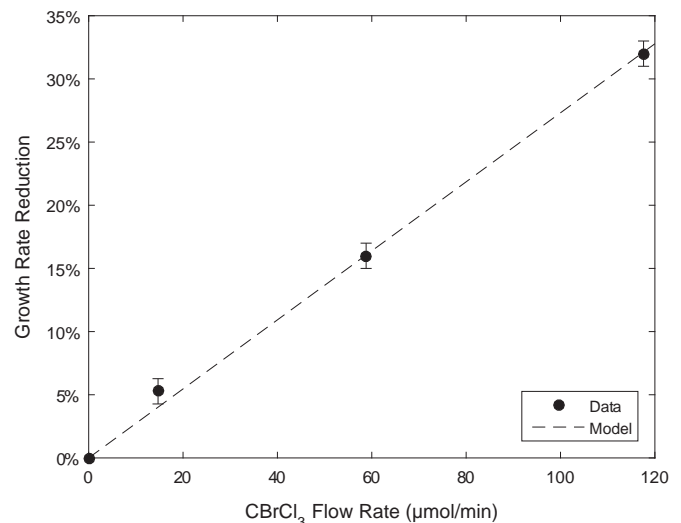

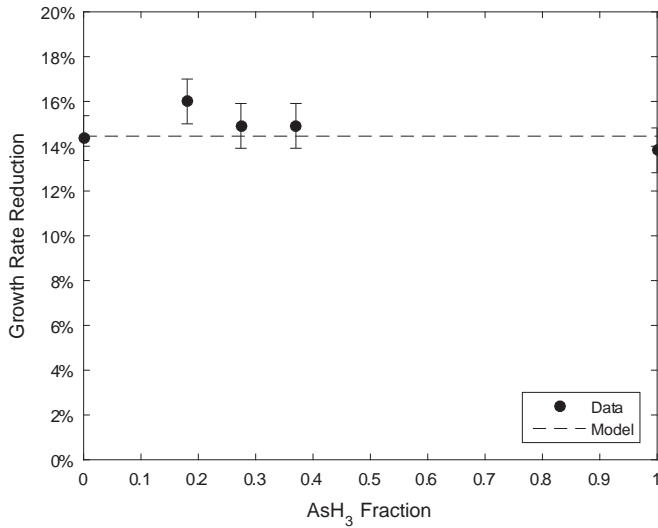**Fig. 2.** Reduction in GaAsP growth rate as a function of CBrCl$_3$ flow rate.

Fig. 3. Reduction in GaAsP growth rate as a function of AsH$_3$ fraction.

growth rate reduction of GaAs by CCl$_4$ as:

$$r = k_0 \left[CX_4 \right] [V/III]^{-0.5} \exp\left(-\frac{E_a}{kT} \right),$$

(2)

where [CX$_4$] is the concentration of C precursor (CCl$_4$ in Lee et al.), E_a is the activation energy of formation of GaCl from Ga and Cl, and k_0 is a constant dependent on other factors [12]. The proportional dependence on C precursor concentration agrees with our data for GaAsP, suggesting that the growth rate reduction is caused by reaction of either Cl or Br byproducts with Ga or Ga precursor.

Growth rate reduction does not change appreciably with AsH$_3$ fraction at a constant CBrCl$_3$ flow rate, as shown in Fig. 3. This is further evidence that the growth rate reduction is limited by the reaction of Br or Cl byproducts with Ga, and that group V species are not involved.

3.3. GaAs$_x$P$_{1-x}$ Composition Shift due to CBrCl$_3$

Fig. 4a shows the GaAs$_x$P$_{1-x}$ composition (x) with a constant AsH$_3$ fraction of 0.2 and a varying CBrCl$_3$ flow. The introduction of CBrCl$_3$ increases the As fraction in the solid phase (x). This trend was also observed by Tateno et al. for InGaAsP doped by CBr$_4$ [13]. The shift in x is approximately the same for all CBrCl$_3$ flows tested (15–118 µmol/min).

The incorporation of high amounts of C is expected to have an effect on the GaAsP lattice constant due to Vegard's Law [21]. However, this shift would be opposite in sign to the shift observed here, that is, towards smaller rather than larger lattice constants. In addition, the magnitude of the shift due to C incorporation is expected to be a small fraction ($<$ 10%) of the observed shift, so it is ignored here.

GaAs$_x$P$_{1-x}$ composition (x) versus AsH$_3$ fraction is shown in Fig. 4b for both no CBrCl$_3$ and for a CBrCl$_3$ flow of 59 µmol/min. Smeets et al. model the relationship between the input partial pressures of AsH$_3$ and PH$_3$ and x as:

$$\frac{1-x}{x} = C \frac{P_{PH_3}}{P_{AsH_3}},$$

(3)

where C is a fitting constant with an Arrhenius dependence and an activation energy close to that of the PH$_3$ cracking energy [22]. For the case of no CBrCl$_3$, this equation fits the data well with C equal to 0.075. For a CBrCl$_3$ flow of 59 µmol/min, the data is well-fit with an adjusted C of 0.066. Eq. 3 with both values for C is plotted in Fig. 4b. This modified model suggests that the CBrCl$_3$ is slowing the PH$_3$ cracking or otherwise consuming a certain fraction of PH$_3$, reducing the amount of elemental P available to enter the film. This could be due to formation of PCl$_3$, PBr$_3$, or similar species.

3.4. Carrier concentration and mobility

Room-temperature hole concentration and mobility versus CBrCl$_3$ flow rate with a fixed AsH$_3$ fraction (0.18) are shown in Fig. 5. A saturation of hole concentration at 2×10^{19} cm^{-3} is observed at high CBrCl$_3$ flow rates. The C concentration of Sample H (AsH$_3$ fraction of 0.18 and CBrCl$_3$ flow rate of 118 µmol/min) was
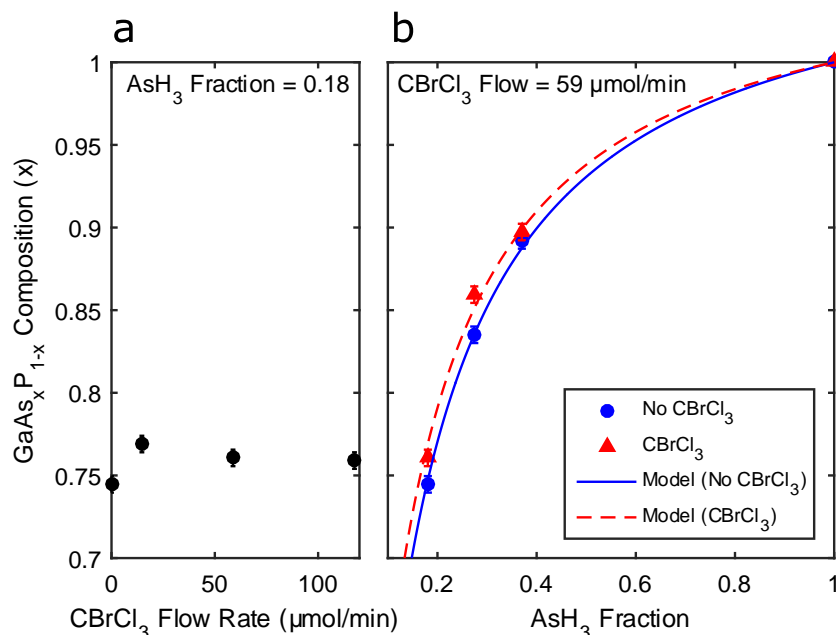

Fig. 4. GaAsP composition (As fraction) versus (a) CBrCl$_3$ flow rate and (b) AsH$_3$ fraction.
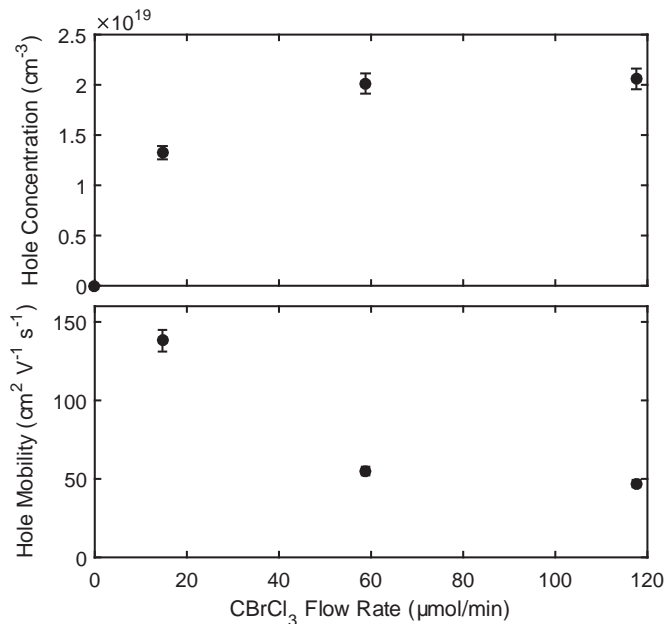
Fig. 5. Hole concentration and mobility versus $CBrCl_3$ flow rate with a fixed AsH_3 fraction (0.18).
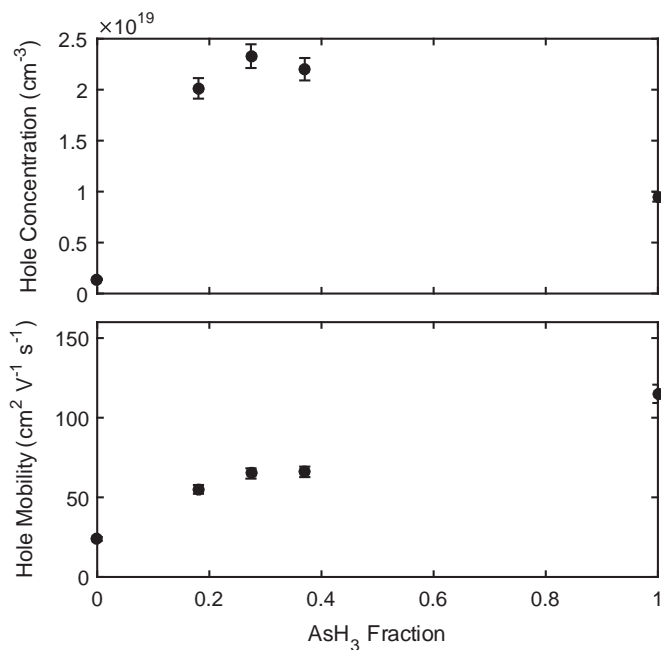

Fig. 6. Hole concentration and mobility versus AsH_3 fraction with a fixed $CBrCl_3$ flow rate (50 μmol/min).

measured by SIMS to be 4×10^{19} cm^{-3} $\pm$ 1×10^{19} cm^{-3}, corresponding to a dopant activation near 50%. The error in C concentration is large because of the unknown matrix effects of GaAsP compared to available GaAs standards. The dopant activation level of near 50% suggests that the saturation in hole concentration is due to a combination of multiple factors: a limitation in incorporation of C into the GaAsP film along with a reduction in dopant activation.

Fig. 6 shows the room-temperature hole concentration and mobility as a function of AsH_3 fraction with a constant $CBrCl_3$ flow rate of 59 μmol/min. Hole concentrations for the three GaAsP samples are similar, while that of the GaAs and GaP samples are lower. Hole mobility increases almost linearly with increasing

AsH_3 fraction. This behavior could be due to a decrease in hole effective mass with increasing As concentration in combination with changing amounts of dopant scattering from incorporated C.

4. Conclusions

We found that $CBrCl_3$ can be used to grow GaAsP at a range of compositions with heavy p-type doping via MOCVD. The growth rate reduction of GaAsP due to $CBrCl_3$ was found to be proportional to $CBrCl_3$ flow rate and constant across GaAsP composition. This suggests that like for GaAs, the growth rate reduction is caused by the formation of GaCl or GaBr. GaAsP composition shifts towards GaAs due to $CBrCl_3$, and was modeled using an adjusted equation from Smeets et al. By accounting for the growth rate and composition shifts, C-doped GaAsP films can be grown with the required precision. Hole concentrations of greater than 2×10^{19} cm^{-3} were achieved across a range of compositions with a $CBrCl_3$ flow rate of 59 μmol/min. At higher $CBrCl_3$ flows, the hole concentration saturated. Hole mobility increased linearly with increasing AsH_3 fraction.

References

[1] A. Bergh, P.J. Dean, Light-emitting diodes, Proc. IEEE. 60 (1972) 156–223.
[2] M.G. Craford, W.O. Groves, Vapor phase epitaxial materials for LED applications, Proc. IEEE. 61 (1973) 862–880.
[3] M. Ohkubo, N. Ikeda, T. Ninomiya, Graded-GaAs$_{1-x}$P$_x$ base in heterojunction bipolar transistors with InGaP emitters, Indium Phosphide Relat. Mater. (1995) 456–459.
[4] T.J. Grassman, M.R. Brenner, M. Gonzalez, A.M. Carlin, R.R. Unocic, R.R. Dehoff, et al., Characterization of metamorphic GaAsP/Si materials and devices for photovoltaic applications, IEEE Trans. Electron Devices 57 (2010) 3361–3369, http://dx.doi.org/10.1109/TED.2010.2082310.
[5] K.N. Yaung, J.R. Lang, M.L. Lee, N. Haven, Towards high efficiency GaAsP solar cells on (001) GaP/Si, in: Photovolt. Spec. Conf. (PVSC), 2014 IEEE 40th, 2014: pp. 831–835. http://dx.doi.org/10.1109/PVSC.2014.6925043.
[6] T. Milakovich, R. Shah, S. Hadi, M. Bulsara, A. Nayfeh, Growth and characterization of GaAsP top cells for high efficiency III-V / Si tandem PV, in: Photovolt. Spec. Conf. (PVSC), 2015 IEEE 42nd, 2015: pp. 1–4. http://dx.doi.org/10.1109/PVSC.2015.7355598.
[7] B.T. Cunningham, L.J. Guido, J.E. Baker, J.S.M. Jr, N.H. Jr., G.E. Stillman, Carbon diffusion in undoped, n-type, and p-type GaAs, Appl. Phys. Lett. 55 (1989) 687–689, http://dx.doi.org/10.1063/1.101822.
[8] M. Konagai, T. Yamada, T. Akatsuka, K. Saito, E. Tokumitsu, K. Takahashi, Metallic p-type GaAs and GaAlAs grown by metalorganic molecular beam epitaxy, J. Cryst. Growth 98 (1989) 167–173.
[9] H. Zhu, Y. Adachi, T. Ikoma, Deep levels in MOCVD GaAs grown under different Ga/As mol fractions, J. Cryst. Growth 55 (1981) 154–163.
[10] M. Kushibe, K. Eguchi, M. Funamizu, Y. Ohba, Heavy carbon doping in metalorganic chemical vapor deposition for GaAs using a low V/III ratio, Appl. Phys. Lett. 56 (1990) 1248, http://dx.doi.org/10.1063/1.103181.
[11] B.T. Cunningham, M.A. Haase, M.J. McCollum, J.E. Baker, G.E. Stillman, Heavy carbon doping of metalorganic chemical vapor deposition grown GaAs using carbon tetrachloride, Appl. Phys. Lett. 54 (1989) 1905–1907, http://dx.doi.org/10.1063/1.101237.
[12] J.-S. Lee, I. Kim, B.-D. Choe, W.G. Jeong, Carbon doping and growth rate reduction by CCl4 during metalorganic chemical-vapor deposition of GaAs, J. Appl. Phys. 76 (1994) 5079–5084, http://dx.doi.org/10.1063/1.357219.
[13] K. Tateno, C. Amano, Carbon doping and etching in Ga$_x$In$_{1-x}$As$_y$P$_{1-y}$ on GaAs substrates using CBr4 by metalorganic chemical vapor deposition, J. Electron. Mater. 28 (1999) 63–68, http://dx.doi.org/10.1007/s11664-999-0196-6.

[14] Y. Bolkhovityanov, O. Pchelyakov, GaAs epitaxy on Si substrates: modern status of research and engineering, Phys. Uspekhi 51 (2008) 437–456, http://dx.doi.org/10.3367/UFNr.0178.200805b.0459.

[15] M.T. Currie, S.B. Samavedam, T.A. Langdo, C.W. Leitz, E.A. Fitzgerald, Controlling threading dislocation densities in Ge on Si using graded SiGe layers and chemical-mechanical polishing, Appl. Phys. Lett. 72 (1998) 1718–1720, http://dx.doi.org/10.1063/1.121162.

[16] I. Vurgaftman, J.R. Meyer, L.R. Ram-Mohan, Band parameters for III–V compound semiconductors and their alloys, J. Appl. Phys. 89 (2001) 5815, http://dx.doi.org/10.1063/1.1368156.

[17] T. Roesener, V. Klinger, C. Weuffen, D. Lackner, F. Dimroth, Determination of heteroepitaxial layer relaxation at growth temperature from room temperature X-ray reciprocal space maps, J. Cryst. Growth 368 (2013) 21–28, http://dx.doi.org/10.1016/j.jcrysgro.2013.01.007.

[18] R. Chwang, B.J. Smith, C.R. Crowell, Contact size effects on the Van Der Pauw method for resistivity and Hall coefficient measurement, Solid State Electron. 17 (1974) 1217–1227, http://dx.doi.org/10.1016/0038-1101(74)90001-X.

[19] M. Kondo, T. Tanahashi, Dependence of carbon incorporation on crystallographic orientation during metalorganic vapor phase epitaxy of GaAs and AlGaAs, J. Cryst. Growth 145 (1994) 390–396, http://dx.doi.org/10.1016/0022-0248(94)91081-2.

[20] C.A. Larsen, N.I. Buchan, G.B. Stringfellow, Mass spectrometric studies of phosphine pyrolysis and OMVPE growth of InP, J. Cryst. Growth 85 (1987) 148–153.

[21] M.C. Hanna, Z.H. Lu, A. Majerfeld, Very high carbon incorporation in metalorganic vapor phase epitaxy of heavily doped p-type GaAs, Appl. Phys. Lett. 58 (1991) 164–166, http://dx.doi.org/10.1063/1.104960.

[22] E.T.J.M. Smeets, Solid composition of $GaAs_{1-x}P_x$ grown by organometallic vapour phase epitaxy, J. Cryst. Growth 82 (1987) 385–395.